Theoretical study on the diradical characters and third-order nonlinear optical properties of transition-metal heterodinuclear systems

4 AUTHORS, INCLUDING:

Benoît Champagne
University of Namur
401 PUBLICATIONS **8,753** CITATIONS

SEE PROFILE

Masayoshi Nakano
Osaka University
337 PUBLICATIONS **4,794** CITATIONS

SEE PROFILE

CrossMark

Theoretical study on the diradical characters and third-order nonlinear optical properties of transition-metal heterodinuclear systems

Taishi Yamada [a], Yudai Inoue [a], Benoît Champagne [b], Masayoshi Nakano [a,*]

[a] Department of Materials Engineering Science, Graduate School of Engineering Science, Osaka University, Toyonaka, Osaka 560-8531, Japan
[b] Laboratoire de Chimie Théorique, University of Namur, rue de Bruxelles, 61, B-5000 Namur, Belgium

ARTICLE INFO

ABSTRACT

We investigate the correlation between the diradical characters and the second hyperpolarizabilities (γ) of several transition-metal heterodinuclear systems using the spin-unrestricted coupled-cluster method. Due to asymmetry, the longitudinal γ values are enhanced by the primary contribution of the dσ electrons with intermediate diradical character. In particular, large enhancements of γ amplitudes and/or change of signs are found for the systems composed of different group metal atoms due to the large asymmetric charge distribution originating from the difference in their ionization potentials. This result indicates a possibility of a novel class of efficient nonlinear optical materials based on transition-metal heterodinuclear complexes.

1. Introduction

Molecular design of highly active third-order nonlinear optical (NLO) materials has been a hot topic in materials science because of their future applications in photonics and optoelectronics including ultra-capacity optical memory [1,2], ultrafast optical switching [3], fabrication of hyperfine structures [4] and so on. Although various types of molecular systems with large third-order NLO properties (or second hyperpolarizability γ at the molecular scale) have been designed both experimentally and theoretically [5–9], there remains space for further enhancing γ, as suggested by the fundamental limits obtained using the Thomas–Kuhn sum rule [10]. As a possible design principle for achieving remarkable γ values, we have theoretically demonstrated that open-shell singlet systems with intermediate diradical characters exhibit larger γ values than closed-shell and pure diradical systems of similar size [11–13]. These theoretical predictions have been experimentally confirmed by two-photon absorption [14,15] and third-harmonic generation [16] measurements, which have stimulated other experimental and theoretical investigations on the third-order NLO properties of singlet diradical compounds [17–21].

Among open-shell singlet NLO candidates, we have theoretically investigated the open-shell nature of the dσ, dπ, and dδ bonds in transition-metal homodinuclear systems, and have clarified the existence of 'σ-dominant' third-order NLO systems, where weak σ-bonds with intermediate diradical character contribute mostly to the total γ in contrast to conventional π-conjugated NLO systems and where their amplitudes can be controlled by adjusting me-

tal–metal bond lengths and metal elements [22,23]. On the other hand, the introduction of asymmetric charge distributions (asymmetricity) into open-shell singlet systems with intermediate diradical characters, either by the application of an external electric field and/or by the chemical substitution with donor/acceptor, can further enhance the γ values as compared to that in closed-shell systems. This has been predicted using the two-site diradical model [24] as well as quantum chemical calculations for donor/acceptor-substituted diphenalenyl compounds [25]. In this Letter, using the spin-unrestricted coupled-cluster singles and doubles (UCCSD) method, we investigate the asymmetricity effects on the open-shell character of the multiple bonds and on the γ values of transition-metal heterodinuclear systems having different bond lengths. This study contributes to revealing the relationships between the structure and third-order NLO property in transition-metal heterodinuclear systems, and subsequently demonstrates their high potential as components in highly active and tunable NLO materials.

2. Model systems and calculation methods

As prototypical model heterodimetallic systems, we investigate Cr(II)—Mo(II) and Cr(II)—Mn(III), which are composed of transition metal atoms of the same group but different period or of the same period but different group, respectively. These models are expected to be useful for clarifying a correlation between y, the asymmetricity, and γ, and thus for illuminating a way of tuning γ through asymmetricity. Both systems bear one dσ, two equivalent dπ, and one dδ bonds due to d^4–d^4 interactions since the metals in group 6 (Cr, Mo) and 7 (Mn) are dicationic and tricationic, respectively. As a reference homodinuclear system, we considered naked Cr(II)—Cr(II), Mo(II)—Mo(II), and Mn(III)—Mn(III) model systems.

* Corresponding author. Fax: +81 6 6850 6268.
E-mail address: mnaka@cheng.es.osaka-u.ac.jp (M. Nakano).

Cr(II)–Cr(II) has already been found to exhibit intermediate dσ diradical characters at the equilibrium bond lengths (1.77–2.69 Å) [26,27] of real dichromium(II) complexes, and to show the significant enhancement of γ values in those region [22,23]. As an extension of the above systems, we also examine the Cr(II)–Tc(III) model system built from transition metal atoms of both different group and different period as well as the corresponding homodinuclear system Tc(III)–Tc(III). Furthermore, Mo(II)–Tc(III) and Mo(II)–Mn(III) are examined as systems exhibiting strong asymmetricity (see Section 3.2).

In all calculations, the effective core potential (ECP) of the Stuttgart group, which includes relativistic effects, was employed together with the corresponding valence basis set (SDD) for Cr and Mn [28] of period 4. For Mo belonging to period 5, the SDD basis set [29] was supplemented with a set of f polarization functions [30] (referred to as 'SDD(f)' in this Letter). This is required to get a balanced basis set because, unlike transition metals of period 4, the SDD basis set for those of higher periods ($\geqslant$5) do not include f polarization functions. These basis sets were found to be sufficient for obtaining quantitative γ values of transition metal–metal bonded systems at the UCCSD and UCCSD(T) levels of approximation [22,23].

The diradical character y_i can be approximately defined using the spin-projected occupation numbers of the spin-unrestricted Hartree–Fock natural orbitals (UNOs) [31]:

$$y_i = 1 - \frac{2T_i}{1 + T_i^2}, \text{ where } T_i = \frac{n_{\mathrm{HONO}-i} - n_{\mathrm{LUNO}+i}}{2}. \tag{1}$$

Here, $n_{\mathrm{HONO}-i}$ and $n_{\mathrm{LUNO}+i}$ are the occupation numbers of the highest occupied natural orbitals (HONO)$-i$ and the lowest unoccupied natural orbitals (LUNO)$+i$ (where i = 0, 1, …), respectively. y_i values range between 0 and 1, which represent closed-shell and pure diradical states, respectively. In the present study, the diradical character associated with the dX orbital [$y(\mathrm{d}X)$, where $X = \sigma$, π, and δ] is obtained using Eq. (1) and the occupation numbers of the corresponding dX bonding and anti-bonding NO pairs. It has been shown to well reproduce the diradical character calculated by other methods such as ab initio configuration interaction (CI) [32] and UCCSD [22] methods.

The static longitudinal γ_{zzzz} ($\equiv \gamma$) values were calculated at the UCCSD level of approximation using the finite-field (FF) approach [33], which consists in a fourth-order differentiation of the energy with respect to the applied electric field. The power series expansion convention (called B convention [34]) was chosen for defining γ. A tight convergence threshold of 10^{-10} a.u. was used on the energy to obtain precise γ values. γ was partitioned into its $\gamma(\mathrm{d}X)$ contributions, calculated from the corresponding $\gamma(\mathrm{d}X)$ density [$d^{\mathrm{d}X(3)}(\mathbf{r})$] [35]:

$$\gamma(\mathrm{d}X) = -\frac{1}{3!} \int r d^{\mathrm{d}X(3)}(\mathbf{r}) d\mathbf{r}, \tag{2}$$

where $d^{\mathrm{d}X(3)}(\mathbf{r})$ is the third-order electric field derivative of the electron density, referred to as $\gamma(\mathrm{d}X)$ density [34], of the bonding (dX) and antibonding (dX^*) NO pair and it reads

$$d^{\mathrm{d}X(3)}(\mathbf{r}) = \frac{\partial^3}{\partial F^3} \{ n_{\mathrm{d}X} \phi^*_{\mathrm{d}X}(\mathbf{r}) \phi_{\mathrm{d}X}(\mathbf{r}) + n_{\mathrm{d}X^*} \phi^*_{\mathrm{d}X^*}(\mathbf{r}) \phi_{\mathrm{d}X^*}(\mathbf{r}) \}|_{F=0}. \tag{3}$$

Here, $\phi_{\mathrm{d}X}(\mathrm{r})$ and $n_{\mathrm{d}X}$ represent the dX NO and its occupation number, respectively. All calculations were performed with the GAUSSIAN 09 program package [36].

3. Results and discussion

3.1. Bond length dependences of $y(\mathrm{d}X)$ and $\gamma(\mathrm{d}X)$ ($X = \sigma$, π, and δ)

Figure 1 shows the bond length (R) dependences of the UHF $y(\mathrm{d}X)$ and UCCSD γ [as well as $\gamma(\mathrm{d}X)$] ($X = \sigma$, π, and δ) for Cr(II)–Mo(II) (a, b) and Cr(II)–Mn(III) (c, d). All $y(\mathrm{d}X)$ increase with R due to decreasing d–d orbital overlaps, and they follow the order $y(\mathrm{d}\delta) > y(\mathrm{d}\pi) > y(\mathrm{d}\sigma)$ at any R (> $\sim$1.8 Å). Besides, each $\gamma(\mathrm{d}X)$ increases in the intermediate $y(\mathrm{d}X)$ region and $\gamma(\mathrm{d}\sigma)$ brings the dominant contribution to γ at R > $\sim$2.0 Å. Therefore, Cr(II)–Mo(II) and Cr(II)–Mn(III) are classified as 'σ-dominant' third-order NLO systems like their homodinuclear Cr(II)–Cr(II) and Mo(II)–Mo(II) analogs [22].

3.2. Asymmetric effects on $y(\mathrm{d}\sigma)$ and $\gamma(\mathrm{d}\sigma)$

The asymmetric charge distribution is governed by the relative ionization potentials of the constituent atoms and by the relative formal charges. In order to estimate the relative ionization potentials of these atoms associated with the dσ bonds, we examined the relative energies of the dz^2 orbitals of Cr(II), Mo(II) and Mn(II) in their quintet states, which build the dσ bonds in the dinuclear systems. At the UHF level, the dz^2 orbital energies are in the order: Mo(II) (-0.9947 a.u.) > Cr(II) (-1.1752 a.u.) > Mn(III) (-1.9473 a.u.), highlighting that Cr(II)–Mn(III) is more asymmetric than Cr(II)–Mo(II) because the orbital energy difference is larger ($\Delta\varepsilon = 0.7721$ a.u. versus 0.1805 a.u.). This is confirmed by the UHF natural population analysis describing a charge transfer of 0.0918e from Mo(II) to Cr(II) in Cr(II)–Mo(II) and a charge transfer of 0.1988e from Cr(II) to Mn(III) in Cr(II)–Mn(III) for R = 2.2 Å. Note that contrary to Mulliken and Löwdin population analysis, the NPA charges reproduce the more reliable Hirshfeld charges [37], (see Supplementary data).

Figure 2a and b shows the R dependences of $y(\mathrm{d}\sigma)$ and $\gamma(\mathrm{d}\sigma)$ of Cr(II)–Mo(II) in comparison to those of their corresponding homodinuclear systems [Cr(II)–Cr(II), Mo(II)–Mo(II)]. At any R
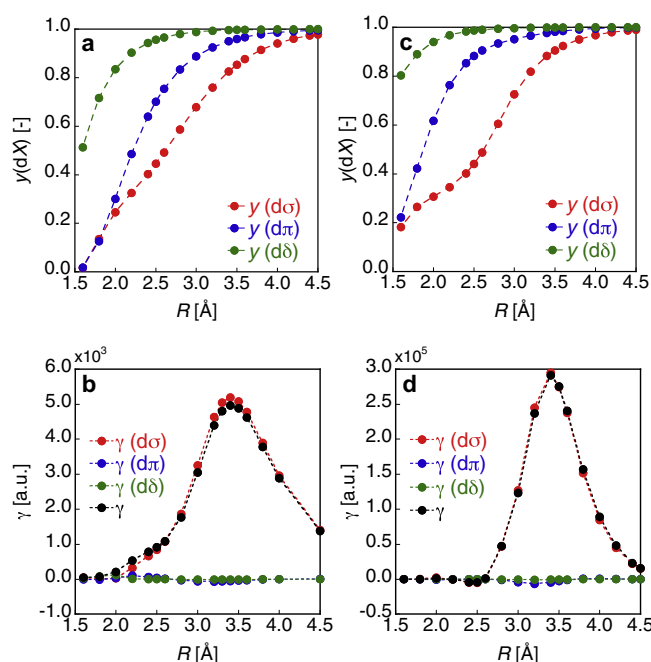

Figure 1. Bond length (R) dependences of $y(\mathrm{d}X)$ and γ [as well as $\gamma(\mathrm{d}X)$] ($X = \sigma$, π, and δ) obtained by the UHF and UCCSD methods, respectively, for Cr(II)–Mo(II) (a, b) and Cr(II)–Mn(III) (c, d).
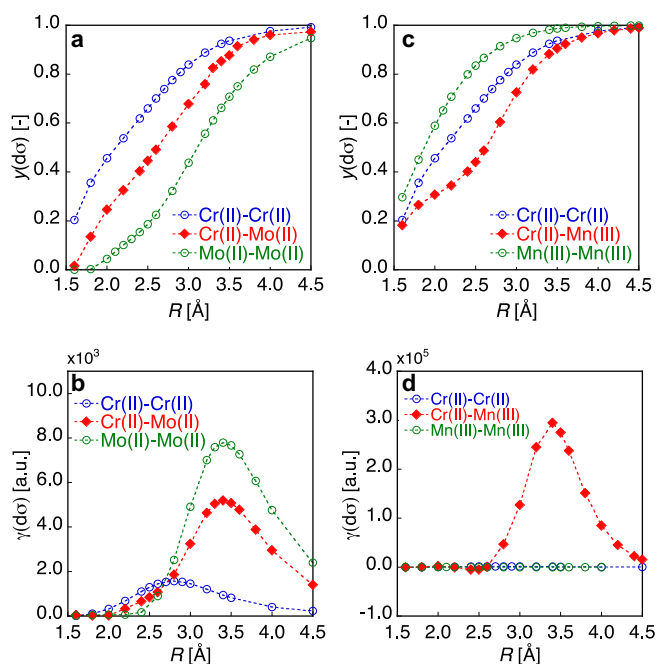
Figure 2. Bond length (R) dependence of $y(d\sigma)$ (a) and $\gamma(d\sigma)$ (b) of Cr(II)–Mo(II) as well as of the corresponding two analogous homodinuclear systems [Cr(II)–Cr(II), Mo(II)–Mo(II)]. Similar plots of Cr(II)–Mn(II) as well as of Cr(II)–Cr(II) and Mn(II)–Mn(II) are shown in (c, d).

$y(d\sigma)$ of Cr(II)–Mo(II) lies between those of Cr(II)–Cr(II) and Mo(II)–Mo(II), and the maximum $\gamma(d\sigma)$ value [$\gamma_{max}(d\sigma)$] is also intermediate. In comparison to the significant changes in y and γ that are observed in open-shell singlet systems under strong electric fields [24,25], this indicates that the asymmetric effect on $y(d\sigma)$ and $\gamma(d\sigma)$ is fairly small in Cr(II)–Mo(II). This result is attributed to the relatively small difference in the atomic ionization potentials.

In contrast to Cr(II)–Mo(II), at any R, the $y(d\sigma)$ of Cr(II)–Mn(III) (Figure 2c) lies below those of its homodinuclear analogs, Cr(II)–Cr(II) and Mn(II)–Mn(II), which is associated with the stronger ionic bond [24]. Furthermore, the $\gamma_{max}(d\sigma)$ of Cr(II)–Mn(III) is substantially enhanced as compared to those of its homodinuclear analogs (see Figure 2d): $\gamma_{max}(d\sigma)$ of Cr(II)–Mn(III) is about 190 times as large as that of Cr(II)–Cr(II) and about 2×10^3 times larger than that of Mn(III)–Mn(III) (see Table 1). This remarkable enhancement of γ is similar to that observed in the open-shell singlet systems under strong electric fields and/or with strong donor/ acceptor substituents, which cause large asymmetric charge distributions [24,25].

3.3. Extension to Cr(II)–Tc(III) system: different group and different period metals

Although complexes involving the Cr(II)–Mo(II) system exist [38–40], those involving Cr(II)–Mn(III) as well as the correspond-

ing homodinuclear system, Mn(III)–Mn(III), have not yet been synthesized. By contrast, complexes involving the Tc(III)–Tc(III) system have been prepared [41–43], which gave us the impetus to examine the Cr(II)–Tc(III) model system. It is predicted that Cr(II)–Tc(III) is less asymmetric than Cr(II)–Mn(III) because the dz^2 orbital energy of Tc(III) (−1.5698 a.u.) is higher than that of Mn(III) (−1.9473 a.u.) and the charge transfer amount from Cr(II) to Tc(III) in Cr(II)–Tc(III) (at $R = 2.2$ Å) goes down to 0.1460e. So, the asymmetricity of Cr(II)–Tc(III) lies between those of Cr(II)–Mo(II) and Cr(II)–Mn(III). This figures out an enhancement of $\gamma_{max}(d\sigma)$ in Cr(II)–Tc(III) with respect to the corresponding homodinuclear systems smaller than in Cr(II)–Mn(III) but larger than in Cr(II)–Mo(II).

From Figure 3a and b, Cr(II)–Tc(III) shows qualitatively the same R dependences of UHF $y(dX)$ and CCSD $\gamma(dX)$ as those of Cr(II)–Mo(II) and Cr(II)–Mn(III) except for the small peak in $y(d\sigma)$ of Cr(II)–Tc(III) around $R = \sim 2.2$ Å. Then, for the whole R range, $y(d\sigma)$ of Cr(II)–Tc(III) is systematically smaller than that of Cr(II)–Cr(II) but very close to that of Tc(III)–Tc(III), especially when $R > \sim 2.2$ Å (Figure 3c). This originates from the smaller diradical character of Tc(III)–Tc(III) than of Mn(III)–Mn(III) (at a given R), because the $d\sigma$ orbitals of Tc(III) are more extended than in Mn(III) [23]. Note that the presence of the small peak in $y(d\sigma)$ for Cr(II)–Tc(III) can be explained by the node structure of the $d\sigma$ atomic orbitals leading to both bonding and anti-bonding overlaps at small inter-atomic distance. Namely, the dz^2 orbital composing the $d\sigma$ orbital presents an antiphase ring distribution unlike the $p\sigma$ molecular orbital built from p_z atomic orbitals. When two dz^2 orbitals get closer, their overlap first increases but then decreases due to the anti-bonding interactions involving the antiphase rings. We thus predict that the overlap decrease in the short R region (between 2.0 and 2.5 Å) is enlarged when the asymmetricity and, subsequently, the difference in size of the dz^2 orbitals in heterodinuclear systems gets more significant. This effect is obvious in Cr(II)–Tc(III) but slightly smaller for Cr(II)–Mn(III), where it results only in a shoulder.

Furthermore, similar to the Cr(II)–Mn(III) case, the $\gamma_{max}(d\sigma)$ of Cr(II)–Tc(III) is remarkably enhanced as compared to those of its
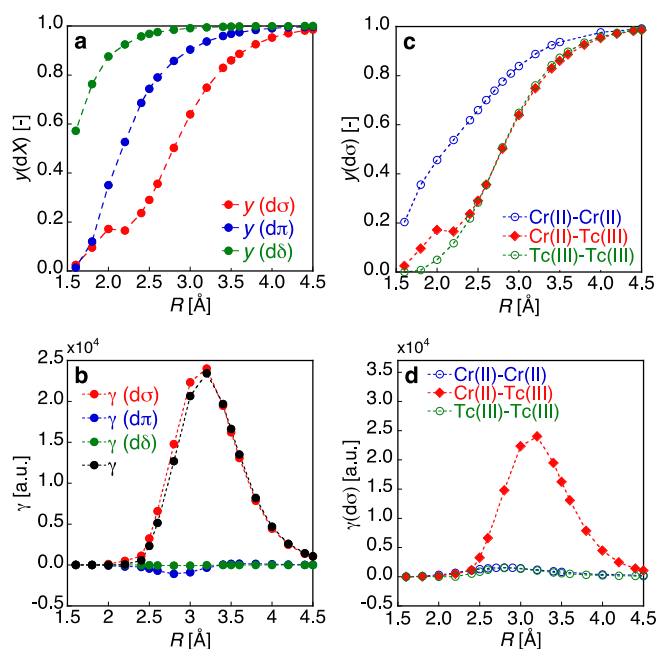

Figure 3. Bond length (R) dependences of $y(dX)$ and γ [as well as $\gamma(dX)$] ($X = \sigma$, π, and δ) obtained by the UHF and UCCSD methods, respectively, for Cr(II)–Tc(II) (a, b). Comparison with the R dependences of $y(d\sigma)$ (c) and $\gamma(d\sigma)$ (d) between Cr(II)–Cr(II), Cr(II)–Tc(III), and Tc(III)–Tc(III).

Table 1
Maximum $\gamma(d\sigma)$ [$\gamma_{max}(d\sigma)$] and γ_{max} as well as the bond length (R_{max}) giving $\gamma_{max}(d\sigma)$ for Cr(II)–Mn(III), Cr(II)–Cr(II) and Mn(III)–Mn(III).

	$\gamma(d\sigma)_{max}$ [$\times 10^3$ a.u.]	γ_{max} [$\times 10^3$ a.u.]	R_{max} [Å]
Cr(II)–Cr(II)	1.57	1.56	2.8
Cr(II)–Mn(III)	295	291	3.4
Mn(III)–Mn(III)	0.133	0.173	2.1

Table 2
Maximum $\gamma(d\sigma)$ [$\gamma_{max}(d\sigma)$] and γ_{max} as well as the bond length (R_{max}) giving $\gamma_{max}(d\sigma)$ for Cr(II)–Tc(III), Cr(II)–Cr(II), Tc(III)–Tc(III), and Mo(II)–Tc(III).

	$\gamma(d\sigma)_{max}$ [$\times 10^3$ a.u.]	γ_{max} [$\times 10^3$ a.u.]	R_{max} [Å]
Cr(II)–Cr(II)	1.57	1.56	2.8
Cr(II)–Tc(III)	24.0	23.5	3.2
Tc(III)–Tc(III)	1.49	1.64	2.8
Mo(II)–Tc(III)	3670	3650	4.2

homodinuclear analogs, Cr(II)–Cr(II) and Tc(III)–Tc(III) (Figure 3d). However, the increase ratios of $\gamma_{max}(d\sigma)$, [Cr(II)–Tc(III)]/[Cr(II)–Cr(II)] and [Cr(II)–Tc(III)]/[Tc(III)–Tc(III)], amount to 15–16 (Table 2), which are much smaller than those of [Cr(II)–Mn(III)]/[Cr(II)-Cr(II)] ~ 190 and [Cr(II)–Mn(III)]/[Mn(III)–Mn(III)] ~ 2 × 10^3. These results are consistent with the interpretation based on the difference of the ionization potentials of the constitutive atoms.

3.4. Extension to Mo(II)–Tc(III) and Mo(II)–Mn(III) system: strong asymmetric case

On the basis of their relative dz^2 ionization potentials, it is predicted that Mo(II)–Tc(III) ($\Delta\varepsilon = 0.5751$ a.u.) has an asymmetricity comparable to Cr(II)–Mn(III) ($\Delta\varepsilon = 0.7721$ a.u.), and that Mo(II)–Mn(III) ($\Delta\varepsilon = 0.9526$ a.u.) has the largest asymmetricity among the examined transition dimetal systems. This is confirmed by the UHF natural population analysis describing a charge transfer of 0.4442e from Mo(II) to Tc(III) in Mo(II)–Tc(III) and a charge transfer of 0.4521e from Mo(II) to Mn(III) in Mo(II)–Mn(III) for $R = 2.2$ Å (cf. a charge transfer of 0.1988e from Cr(II) to Mn(III) in Cr(II)–Mn(III) for $R = 2.2$ Å). It is also noted that at $R = 3.0$ Å, a charge transfer from Mo(II) to Mn(III) in Mo(II)–Mn(III) attains 0.9034e, while that from Mo(II) to Tc(III) in Mo(II)–Tc(III) reduces to 0.3174e, which is smaller than that at $R = 2.2$ Å like in the other dimetals. This indicates that in large R region, Mo(II)–Mn(III) has

an almost ionic ground state, while Mo(II)–Tc(III) a diradical ground state.

Figure 4a and b display the R–y and R–γ plots of Mo(II)–Tc(III). As found for other compounds, the $\gamma(d\sigma)$ contributions are dominant in the intermediate $y(d\sigma)$ region. As compared to Cr(II)–Mn(III) and Cr(II)–Tc(III) (Figure 3), $y(d\sigma)$ increases very slowly with R and the γ_{max} is further enhanced [more than one order of magnitude as compared to Cr(II)–Mn(III)] at a larger ($R_{max} = 4.2$ Å) (see Table 2). This comes from the fact that higher period metals give more expanded dz^2 orbitals, which gives, for a given R, a smaller $y(d\sigma)$ value than for the corresponding lower period metals [23]. In sharp contrast, the further increase in the asymmetricity observed in Mo(II)–Mn(III) leads to negative γ values, the amplitudes of which increase rapidly with R though the $y(d\sigma)$ value is reduced and similar to the Mo(II)–Tc(III) case (see Figure 4c and d). This indicates that the ground state of Mo(II)–Mn(III) is almost an ionic state rather than a singlet diradical. Namely, this result suggests that a too strong asymmetricity gives to the system an almost ionic closed-shell ground state, which leads to a sign reversal of γ and its rapid amplitude increase with R. This feature is similar to that observed for closed-shell systems in the presence of a large external field, where γ gets negative and very large, of larger amplitude than the positive maximum value achieved for smaller asymmetricity [44].

4. Concluding remarks

We have theoretically investigated the bond length dependences of the diradical character $y(dX)$ and second hyperpolarizability γ [as well as $\gamma(dX)$] for Cr(II)–Mo(II), Cr(II)–Mn(III), Cr(II)–Tc(III), Mo(II)–Tc(III), and Mo(II)–Mn(III). With the exception of Mo(II)–Mn(III), these systems show significant enhancements of positive γ, which are dominated by $\gamma(d\sigma)$, in the intermediate $y(d\sigma)$ region, and are classified as 'σ-dominant' open-shell singlet third-order NLO systems. Up to a level of asymmetricity, it is also found that the larger the asymmetricity, reflecting the difference of ionization potentials [Mo(II) < Cr(II) < Tc(III) < Mn(III)], the larger the positive γ in the intermediate $y(d\sigma)$ region. The predicted order of asymmetricity is Cr(II)–Mo(II) < Cr(II)–Tc(III) < Mo(II)–Tc(III) < Cr(II)–Mn(III) < Mo(II)–Mn(III). As a result, for example, the maximum $\gamma(d\sigma)$ of Cr(II)–Mn(III) is significantly enhanced as compared to those of its homodinuclear analogs, while that of Cr(II)–Mo(II) lies in between those of its homodinuclear ones.

These results suggest that the enhancement of $\gamma(d\sigma)$ in the intermediate $y(d\sigma)$ region of the heterodinuclear systems composed of atoms of the same period but of different group is larger than for those of the same group but of different period. Indeed, in another model, Cr(II)–Tc(III), built from atoms both of different group and period, the increase ratio of the maximum $\gamma(d\sigma)$ with respect to those of the corresponding homodinuclear systems is less than for Cr(II)–Mn(III) since the asymmetricity of Cr(II)–Tc(III) lies between those of Cr(II)–Mo(II) and Cr(II)–Mn(III). Furthermore, Mo(II)–Tc(III), which presents both a large asymmetricity (due to the large ionization potential difference) and large R_{max} (due to the higher period metals), exhibits the largest positive γ_{max} among the present dimetal systems. It is here noted that the bond lengths (R_{max}) giving γ_{max} are large but that this is expected to be realized by designing ligands. Indeed, dimetal complexes with large metal–metal bond lengths have been described [45,46]. In contrast, too strong asymmetricity like in Mo(II)–Mn(III) gives an almost ionic ground state, which subsequently strongly reduces y and leads to negative γ with large amplitudes, rapidly increasing with R,

In summary, it is predicted that transition-metal heterodinuclear systems with intermediate $y(d\sigma)$ have the possibility of exhibiting enhanced γ amplitudes and/or of reversing their signs in the
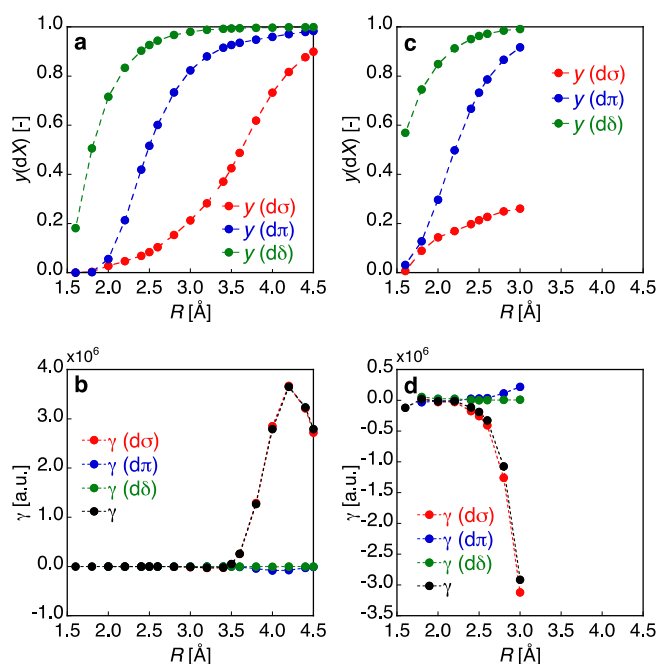

Figure 4. Bond length (R) dependences of $y(dX)$ and γ [as well as $\gamma(dX)$] ($X = \sigma, \pi$, and δ) obtained by the UHF and UCCSD methods, respectively, for Mo(II)–Tc(III) (a, b) and Mo(II)–Mn(III) (c, d). In the case of Mo(II)–Mn(III), no converged self-consistent-field solutions could be obtained beyond $R = 3.0$ Å.

case of a large asymmetricity as compared to those of homodinuclear systems and that this can be controlled by choosing the ionization potentials of the constituent metals.

Acknowledgments

Appendix A. Supplementary data

Supplementary data associated with this article can be found, in the online version, at http://dx.doi.org/10.1016/j.cplett.2013.05.072.

References

[1] D. Day, M. Gu, et al., Adv. Mater. 13 (2001) 1005.
[2] S. Kawata, Y. Kawata, et al., Chem. Rev. 100 (2000) 1777.
[3] S. Tao et al., Adv. Mater. 19 (2007) 2707.
[4] S. Kawata et al., Nature 421 (2001) 697.
[5] Handbook of Advanced Electronic and Photonic Materials and Devices, Nonlinear Optical Materials, edited by H. S. Nalwa (Academic, New York, 2001), Vol. 9.
[6] C.W. Dirk et al., Int. J. Quantum Chem. 43 (1992) 27.
[7] J.L. Brédas et al., Chem. Rev. 94 (1994) 243.
[8] F. Terenziani et al., Adv. Mater. 20 (2008) 4641.
[9] S. Mukhopadhyay et al., Chem. Sci. 3 (2012) 3103.
[10] M.G. Kuzyk, Phys. Rev. Lett. 85 (2000) 1218; erratum 90 (2003) 039902(E).
[11] M. Nakano, R. Kishi, et al., J. Phys. Chem. A 109 (2005) 885.
[12] M. Nakano, R. Kishi, et al., Phys. Rev. Lett. 99 (2007) 033001.
[13] M. Nakano et al., Chem. Phys. Lett. 418 (2006) 142.
[14] K. Kamada, K. Ohta, et al., Angew. Chem. Int. Ed. 46 (2007) 3544.
[15] K. Kamada, S. Fuku-en, et al., J. Am. Chem. Soc. 135 (2013) 232.
[16] H. Kishida, K. Hibino, et al., Thin Solid Films 519 (2010) 1028.
[17] S. Cho, J.M. Lim, et al., J. Am. Chem. Soc. 131 (2009) 6412.
[18] G.S. He, J. Zhu, et al., J. Am. Chem. Soc. 133 (2011) 6675.
[19] M. Ishida, J.-Y. Shin, et al., J. Am. Chem. Soc. 133 (2011) 15533.
[20] Y. Li, W. Heng, et al., J. Am. Chem. Soc. 134 (2012) 14913.
[21] Z. Zeng, Y.M. Sung, et al., J. Am. Chem. Soc. 134 (2012) 14513.
[22] H. Fukui, M. Nakano, et al., J. Phys. Chem. Lett. 2 (2011) 2063.
[23] H. Fukui, Y. Inoue, et al., J. Phys. Chem. A 116 (2012) 5501.
[24] M. Nakano et al., J. Chem. Phys. 133 (2010) 154302.
[25] M. Nakano, T. Minami, et al., J. Phys. Chem. Lett. 2 (2011) 1094.
[26] S. Horvath, S. Gorelsky, et al., Angew. Chem. Int. Ed. 47 (2008) 9937.
[27] F.A. Cotton, C.A. Murillo, et al., Inorg. Chem. 39 (2000) 3728.
[28] M. Dolg, U. Wedig, et al., J. Chem. Phys. 86 (1987) 866.
[29] D. Andrae, U. Haussermann, et al., Theor. Chim. Acta 77 (1990) 123.
[30] A.W. Ehlers, M. Bohme, et al., Chem. Phys. Lett. 208 (1993) 111.
[31] K. Yamaguchi, Chem. Phys. Lett. 33 (1975) 330.
[32] D. Herebian, K.E. Wieghardt, F.J. Neese, Am. Chem. Soc. 125 (2003) 10997.
[33] H.D. Cohen, C.C.J. Roothaan, et al., J. Chem. Phys. 43 (1965) S34.
[34] A. Willetts, J.E. Rice, D.M. Burland, et al., J. Chem. Phys. 97 (1992) 7590.
[35] M. Nakano et al., Theor. Chem. Acc. 130 (2011) 711; erratum 130 (2011) 725.
[36] M.J. Frisch, G.W. Trucks, et al., Gaussian 09, revision A.1, Gaussian, Inc., Wallingford, CT, 2009.
[37] C.F. Guerra et al., J. Comput. Chem. 25 (2004) 189.
[38] C.D. Garner, R.G. Senior, et al., J. Am. Chem. Soc. 98 (1976) 3526.
[39] J.C. Menezes, C.C. Romao, et al., Polyhedron 9 (1990) 1237.
[40] B.E. Bursten, F.A. Cotton, et al., J. Am. Chem. Soc. 101 (1979) 6244.
[41] F.A. Cotton, L. Daniels, et al., Inorg. Chem. 20 (1981) 3051.
[42] F.A. Cotton, L.D. Gage, et al., Nouv. J. Chim. 1 (1977) 441.
[43] S.V. Kryuthchkov, Top. Curr. Chem. 176 (1996) 189.
[44] F. Meyers, J.L. Brédas, J. Zyss, J. Am. Chem. Soc. 114 (1992) 2914.
[45] J.-P. Djukic et al., Eur. J. Inorg. Chem. 1998 (1998) 1781.
[46] S. Tofke et al., J. Organomet. Chem. 338 (1988) 29.